First Sliding Mode Control of a DFIG-based Wind Turbine with mechanical part control

LARBI DJILALI[1], OSCAR J. SUAREZ[1], ALDO PARDO GARCIA[2], MOHAMMED BELKHEIRI[3]
Electrical Engineering Department
[1]CINVESTAV, [2]University of Pamplona, [3]University Amar Telidji
Av. del Bosque 1145-Col. El Bajío, Campus Pamplona, Laghouat
MEXICO, COLOMBIA, ALGERIA
larbidjar@hotmail.com, javier11213@hotmail.com,
apardo13@hotmail.com, m.belkheiri@lagh-univ.dz

Abstract: - The objective of this article is the study of the dynamic behavior of a wind turbine based on doubly fed induction generator (DFIG) with Maximum Power Point Tracking (MPPT) without enslavement of speed and PITCH control. The DFIG stator is directly connected to the grid however; the rotor is linked via a power electronic converter (rectifier, filter, and inverter). The stator active and reactive powers are controlled directly by adjusting the DFIG rotor quantities, while applying direct vector control based on a first order sliding mode controller (SMC).

Key-Words: - Wind turbine, MPPT, PITCH, DFIG, active and reactive power, sliding mode.

1 Introduction

Nowadays, wind energy has many advantages, because it does not pollute and is an inexhaustible source of energy. The performance of a wind turbine depends essentially on three parameters: the power of the wind, the turbine power curve, and the ability of the generator to respond to fluctuations in the wind. The DFIG is a machine which has shown an excellent performance and is widely used in the wind turbine industry [1]. There are many reasons to use a DFIG for variable speed wind turbine, such as reducing stress on the mechanical parts, noise reduction, and the possibility of the active and reactive powers control [1].

A wind system based on DFIG using a 'back-to-back' converter to connect the rotor of the generator with the network presents many advantages; one is being that the power converters are sized to move a fraction of the total power of the system [2]. To maximize this energy, a wind turbine should include [3] [4]:

- A system that allows mechanical control
- A system that allows electrical control

In this article, we present a sliding mode control strategy applied to control; the MPPT algorithm without enslavement of the rotation speed, and PITCH system to control aero-generator. In section 2 the wind turbine modeling is presented. Then, in section 3, the strategy of the command of the mechanical part, including the MPPT algorithm without enslavement of rotational speed and the blade orientation (PITCH) system is studied. In the section 4, the model of the DFIG in the coordinate system (d,q) and vector control based on the SMC of the active and reactive DFIG powers is introduced. We conclude with the presentation of the simulation results.

2 Modeling of the wind turbine

2.1 Modeling of the turbine

The theoretically undisturbed power of the wind through a surface $\boldsymbol{S}$ without loss of speed is [4]:

$$\boldsymbol{P_{wind} = \frac{1}{2}\rho S {v_1}^3} \quad \textbf{(1)}$$

where $\boldsymbol{P_{wind}}$ is the wind power (W) and, $\boldsymbol{\rho}$ is the air volume density (Kg/m^3). Fig 1 presents the horizontal axis wind system where $\boldsymbol{v_1}$ and $\boldsymbol{v_2}$ are upstream and downstream of wind speed, respectively. The tube surface area before and after are given by $\boldsymbol{s_1}$, $\boldsymbol{s_2}$ and the swept area of turbine blades is given by $\boldsymbol{S}$. The equation which expresses the incompressibility of the air and the permanence of flow is written by

$$\boldsymbol{P_{turb} = \frac{1}{2}\rho S v({v_1}^2 - {v_2}^2)} \quad \textbf{(2)}$$

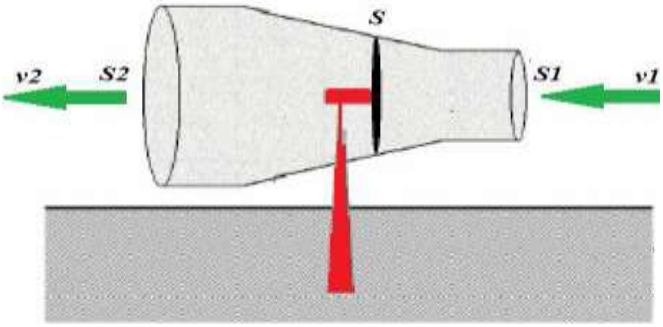

Figure 1. Stream around a wind turbine tube

where P_{turb} is the power extracted by the turbine. When the speed of the air passing through the turbine is given by [5][6],

$$v = \frac{1}{2}(v_1 + v_2) \quad (3)$$

then the ratio between the extracted power of the wind and the total power theoretically available is

$$C_p = \frac{P_{turb}}{P_{wind}} = \frac{1}{2}|1 - (\frac{v_1}{v_2})^2||1 + (\frac{v_1}{v_2})|$$

then,

$$P_{turb} = C_p P_{wind} = \frac{1}{2} C_p \rho S v^3 \quad (4)$$

This is exactly the power absorbed by the wind turbine. From the definition of the relative speed, λ can be found as follows:

$$\lambda = \frac{\Omega_t r}{v} \quad (5)$$

where Ω_t is the turbine's mechanical speed, r is its radius, and v is wind speed. The power coefficient C_p represents the aerodynamic performance of the wind turbine and also depends on the characteristic of the turbine. This factor presents a theoretical limit, called the BETZ limit, which is equal to 0.593 and is not achievable in practice [7].

The study of a particular turbine allowed deducing the following empirical formula for variable speed wind turbines:

$$C_p = C_1\left(C_2\frac{1}{\Lambda} - C_3\beta^x - C_4 - C_5\right)exp\left(\frac{-C_6}{\Lambda}\right) \quad (6)$$

where,

$$C_1 = 0.5;\ C_2 = 116;\ C_3 = 0.4;\ C_4 = 0.4;\ C_5 = 5;$$

$$C_6 = 21;\ \frac{1}{\Lambda} = \frac{1}{\lambda + 0.08\beta} - \frac{0.035}{1+\beta^3}$$

Fig. 2 shows the curves of the power factor λ for different values of blade pitch angle β.We obtain a coefficient of maximum power of 0.3522 for a speed ratio λ equal to 9.7 (λ_{opt}).

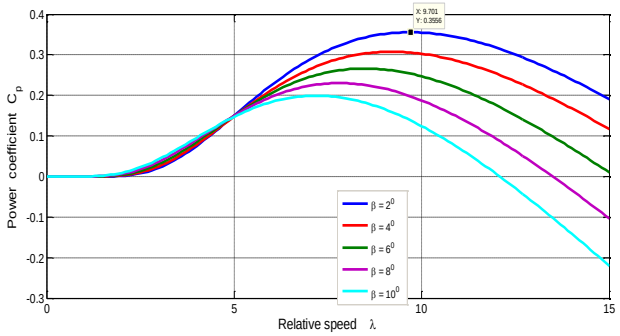

Figure 2. Power based on λ coefficient and β angle

2.2 The multiplier mode

The multiplier is the link between the turbine and the generator. It is assumed to be rigid and modeled by a simple gain [8] [9]:

$$T_{mec} = \frac{1}{G}T_t \quad (7)$$

$$\Omega = G\Omega_t \quad (8)$$

where T_{mec} is mechanical torque (N.m), $T_t$is mechanical torque (N.m) on the axis of the turbine, G is the multiplier gain, Ω is the Mechanical speed (rad/s), and Ω_t is the Turbine mechanical speed (rad/s). We can write the fundamental equation of the mechanical system dynamics of the DFIG as follows:

$$J\frac{d\Omega}{dt} = T_{mec} - T_{em} - f\Omega \quad (9)$$

where **J** is the total inertia of system (Kg.m^2), $T_{em}$is electromechanical torque and, **f** is the coefficient of friction (N.m/s). These equations provide the turbine block diagram in Fig. 3.

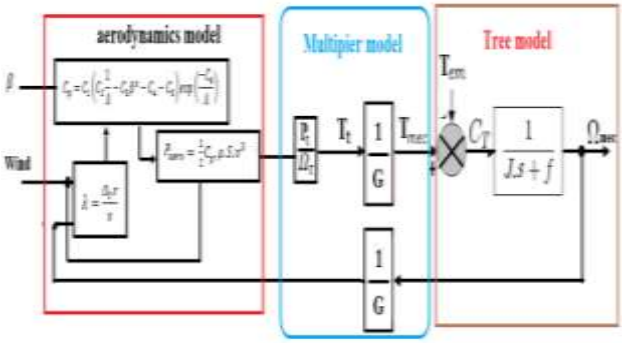

Figure 3. Aerodynamic and mechanical wind turbine model

3 Control of the Mechanical Part

3.1 The MPPT algorithm

The operation of a wind turbine at a variable speed can be defined according to three areas [10] [11], as shown in Fig. 4. In zone 1, the wind speed is low, insufficient to start the turbine. In zone 2, the wind reaches v_{min} , allowing startup. The wind turbine will operate so as to extract the maximum available power MPPT algorithm for optimal operation until the wind reaches v_n. In zone 3, the wind reaches speeds higher than the rated speed; the rotational speed and mechanical power will be maintained at their nominal values so as not to damage the wind turbine. The speed limitation of the aero-generator and the mechanical power generated by the turbine are assured by the PITCH system [11] [12].

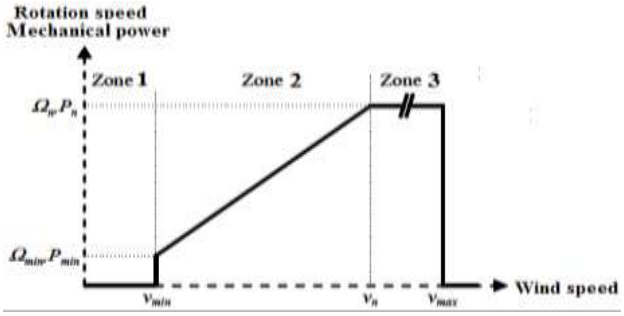

Figure 4. Zones of operation of a wind turbine at variable speed

In practice, a precise measurement of wind speed is difficult to achieve. Therefore, most wind turbines are controlled without enslavement of speed [13]. This command structure is based on the assumption that the wind speed varies very little in a permanent system and based on the following equation:

$$T_{em}^{ref} = \frac{C_{pmax}\rho\pi r^5}{2\lambda_{opt}{}^3 G^3} * \Omega^2 \qquad (10)$$

The structure is shown in Fig. 5.

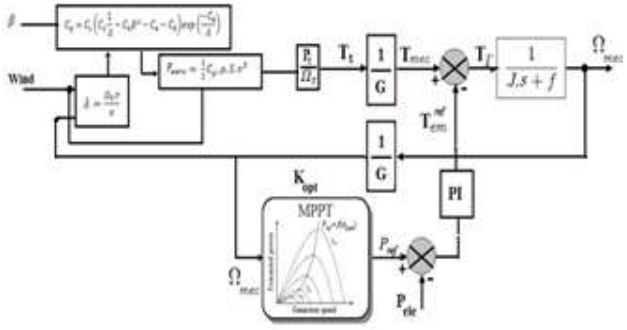

Figure 5. MPPT: control without enslavement of the rotational speed

3.2 Modeling of the PITCH system

Nowadays, high-powered wind turbines use the PITCH system for power control in zone 3. For this purpose, they use the principle of aerodynamic control to limit the extracted power to its nominal value [5]. The PITCH system control reduces the yield when β increases. Fig. 6 shows the different parts of an angle control system.

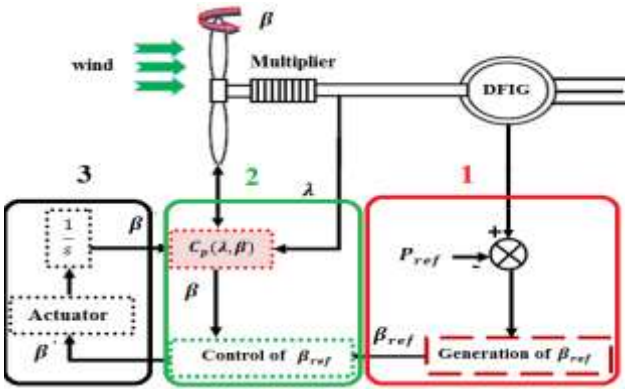

Figure 6. Diagram of the angle control block

4 Modeling and Control of the DFIG

4.1 Modeling of the DFIG

The DFIG can be presented by means of different mathematical models according to the chosen variable states; the model proposed in this manuscript is given by:

$$\mathbf{X} = [\mathbf{I_{sd}}\ \mathbf{I_{sq}}\ \mathbf{\Phi_{rd}}\ \mathbf{\Phi_{rq}}\ ]^{\mathbf{T}} \qquad (11)$$

Therefore, the DFIG model is given by:

$$\dot{I}_{sd} = -\gamma I_{sd} + w_s I_{qs} + \frac{k}{T_r}\Phi_{rd} + k(w_s - w_r)\Phi_{rq} - kV_{rd} + \frac{V_{sd}}{\delta L_s}$$
$$\dot{I}_{sq} = -w_s I_{qs} - \gamma I_{sq} + k(w_r - w_s)\Phi_{rd} - \frac{k}{T_r}\Phi_{rq} - kV_{rq} + \frac{V_{sq}}{\delta L_s}$$
$$\dot{\Phi}_{rd} = \frac{L_m}{L_r} I_{sd} - \frac{1}{T_r}\Phi_{rd} + w_r \Phi_{rq} + V_{rd}$$
$$\dot{\Phi}_{rq} = \frac{L_m}{L_r} I_{sq} - \frac{1}{T_r}\Phi_{rq} - w_r \Phi_{rd} + V_{rq}$$

with:

$$\gamma = \left[\frac{1}{\delta T_s} + \frac{L_m{}^2}{\delta L_s L_r T_r}\right] ;\ T_r = \frac{L_r}{R_r} ; T_s = \frac{L_s}{R_s}$$
$$K = \frac{L_m}{\delta L_s L_r} ;\ \delta = [1 - \frac{L_m{}^2}{L_r L_S}]$$

where $I_{sd}, I_{sq}, \Phi_{rd}$, and Φ_{rq} are the currents and flux of the stator and rotor; V_{sd}, V_{sq}, V_{rd} and V_{rq} are the voltages of the stator and rotor; w_s and w_r are the angular velocities of rotation; L_s and L_r are cyclic

inductances of a stator and rotor phase, respectively; and L_m is the maximum mutual inductance between a stator and rotor phase.

The expression of electromagnetic torque (T_{em}) of the DFIG is written as follows:

$$T_{em} = -\frac{pL_m}{L_r}\left(I_{sq}\Phi_{rd} - I_{sd}\Phi_{rq}\right) \quad (12)$$

The active and reactive power stator of the DFIG is

$$\begin{cases} P_s = V_{sd}I_{sd} + V_{sq}I_{sq} \\ Q_s = V_{sq}I_{sd} - V_{sd}I_{sq} \end{cases}$$

According to the model of active and reactive power, we can see that the strong coupling between two power axes and the electromagnetic torque is the cross-product between stator flux and rotor currents, which makes it particularly difficult to control DFIG. In order to simplify the control of DFIG, we approximate its model to the continuous machine model, applying Filed-orient Control (FOC).
In the FOC model, the DFIG has natural decoupling between two control axes; to apply the proposed method, we take:

$$\Phi_{rd} = \Phi_s \text{ and } \Phi_{sd} = 0$$

So, the electromagnetic torque is written as

$$T_{em} = \frac{pL_m}{L_s}\left(I_{rq}\Phi_{sd}\right) \quad (13)$$

In the field of wind energy production, these are average and high power machines; ignoring the stator resistance and taking the constant stator flux, we can write

$$V_{sd} = 0$$
$$V_{sq} = w_s\Phi_{sd} = V_s$$

Taking into account the simplifications, the expression of the stator powers are

$$P_s = -V_s\frac{L_m}{L_s}I_{rq} \quad (14)$$

$$Q_s = -V_s\frac{L_m}{L_s}I_{rd} + \frac{V_s^2}{L_s w_s} \quad (15)$$

In order to properly control the machine, we then need to establish the relationship between the currents and the rotor voltages that will be applied to the machine [14] [15].

$$V_{rq} = R_r I_{rq} + \sigma L_r\frac{dI_{rq}}{dt} - g w_s \sigma L_r I_{rd} + g\frac{L_m V_s}{L_s} \quad (16)$$

$$V_{rd} = R_r I_{rd} + \sigma L_r\frac{dI_{rd}}{dt} - g w_s \sigma L_r I_{rq} \quad (17)$$

4.2 Application of first order sliding mode control

The advantages of sliding mode control are significant and multiple: high precision, good stability, simplicity, invariance, and robustness. This allows it to be particularly suited to the system with a vague template [15].

In sliding mode theory, the structure control law has two parts:

- A continuous part presents the dynamic of system during the sliding mode.
- A discontinuous part (switching control) presents the dynamic during the convergence mode.

The design of the command can be performed in three major steps, dependent on each other [15] [16].

- Choose the sliding mode surface.
- Find the existing conditions of sliding mode control.
- Determine the law of control.

4.2.1 Control of active power

We apply the expression of Slotine [9] to find the active power sliding surface:

$$S(P_s) = P_{sref} - P_s \quad (18)$$

The derivative of the sliding surface is

$$\dot{S}(P_s) = \dot{P}_{ref} - \dot{P}_s \quad (19)$$

Replacing the expression of active power described by equation (14), we obtain

$$\dot{S}(P_s) = \dot{P}_{sref} + V_s\frac{L_m}{L_s}\dot{I}_{rq} \quad (20)$$

We conclude the expression of the current derivative from equation (16) by compensating the disturbance terms and ignoring the coupling terms between the control axis due to small slip value (g=0.03). We obtain,

$$\dot{S}(P_s) = \dot{P}_{sref} - V_s\frac{L_m}{\sigma L_r L_s}(V_{rq} - R_r I_{rq}) \quad (21)$$

The control algorithm appears in the following equation:

$$\dot{S}(P_s) = \dot{P}_{sref} - V_s \frac{L_m}{\sigma L_r L_s}((V_{rq}^{eq} + V_{rq}^{n}) - R_r I_{rq}) \quad (22)$$

During sliding mode and permanent scheme, the derivative of the surface is zero (because the error is equal to zero), plus attractive control V_{rq}^{n} (which does not exist in this mode). The equivalent control is given by

$$V_{rq}^{eq} = -\frac{\sigma L_r L_s}{V_s . L_m}\dot{P}_{sref} + R_r I_{rq} \quad (23)$$

This command ensures that the trajectory of the controlled quantity remains on its sliding surface. However, this command does not ensure control when the dynamic behavior is not found on the sliding surface. Therefore, it is necessary to add a new condition to ensure that the system state tends towards the surface and reaches it. This new condition is the condition of attractiveness [17] [18] [19].

The sliding mode exists if and only if the following condition is true:

$$S(P_s)\dot{S}(P_s) < 0 \quad (24)$$

During the convergence mode, by replacing the term V_{rq}^{eq} in equation (22), we obtain a new expression of the derivative of the surface, as follows:

$$\dot{S}(P_s) = V_s \frac{L_m}{\sigma L_r L_s} {V_{rq}}^{n} \quad (25)$$

According to the arrival approach [8] (arrival law with a speed of constant arrival), the switching term is given by

$${V_{rq}}^{n} = -Qsign(S(P_s)) \quad (26)$$

4.2.1 Control of reactive power

To control the reactive power, we adapt the same procedure applied in active power control by replacing the symbols P_s, P_{sref}, I_{rq}, and V_{rq}, respectively, with Q_s, Q_{sref}, I_{rd}, and V_{rd}.

5 Simulation Results

The strategy of field-oriented control with a first order sliding mode regulator of stator active and reactive power with power electronic interface using PWM technique has been implemented in the Matlab Simulink* environment to evaluate and test the control of the complete system, as shown in Fig.7. The wind turbine system of 1.5MW is based on DFIG and Table 1 shows the main characteristics of the wind power generation system.

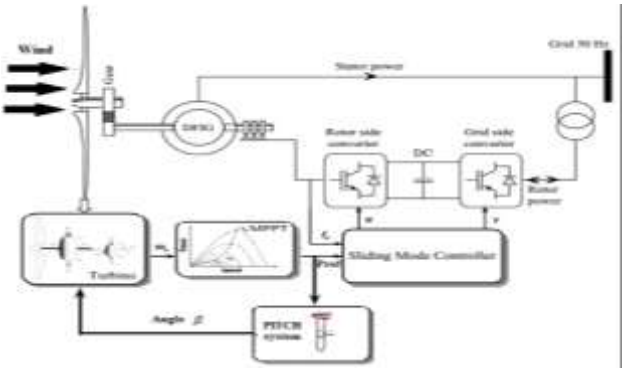

Figure 7. Diagram of the proposed control for Wind turbine system

Designation and symbols		Values
Nominal power.	P_n	1.5 MW
Stator resistance.	R_s	0.012 Ω
Rotor resistance.	R_r	0.021 Ω
Stator inductance.	L_s	0.0137 H
Rotor inductance.	L_r	0.0136 H
Magnetizing inductance.	L_m	0.013 H
Turbine radius.	r	35.25 m
Blades numbers.	-	3
Gain multiplier.	G	90
Total inertia.	J	1000 Kgm^2

Table 1. Parameters of Wind turbine system

Fig. 8 shows the wind speed variation. The wind profile begins with a wind speed equal to the nominal values (15.5m/s). This value is increased after one second to apply the high speed wind values (20 m/s) on the aero generator system to test the PITCH system. At 1.5s, we apply wind speed values lower than the nominal to examine the MPPT algorithm.

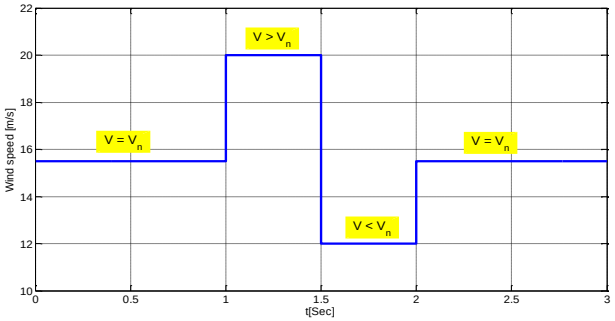

Figure 8. Speed of the wind

*** Simulink, Matlab de © 1994-2015 The Math Works, Inc.**

The main objective of mechanical parts control of a wind turbine system is to extract the maximum existing wind power using the MPPT algorithm when wind speed values are lower than the nominal and to protect the turbine by decreasing the yield when the speed wind is higher than the nominal value using the PITCH system.
Fig. 9 shows the mechanical speed dynamics of the DFIG shaft when the variable amplitude steps of stator active and reactive power were applied.

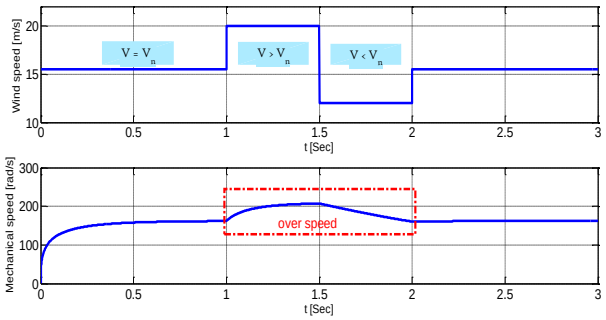

Figure 9. Variations of the wind speed and the mechanical rotation speed without PITCH system and MPPT algorithm peed of the wind

The same reference levels are applied to the DFIG input, but we integrate the mechanical control technique without rotational speed control (Pitch system and MPPT algorithm). Note that mechanical speed variation is controlled, as shown in Fig. 10. When the wind reaches the nominal speed, the mechanical speed reaches its nominal value (163 rad/s). If the wind speed increases, the PITCH system decreases the yield of the wind turbine to keep the nominal value and protect the wind (1−1.5s). When the wind speed decreases, the MPPT algorithm is applied to extract the maximum wind power (1.5−2s).

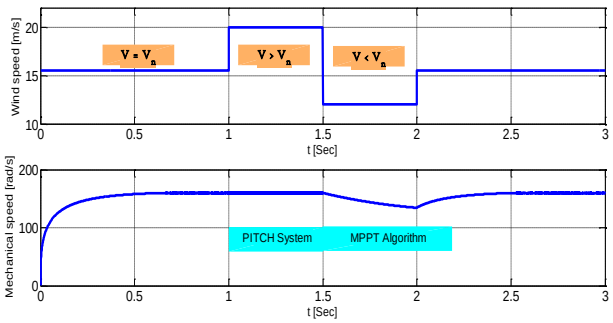

Figure 10. Wind speed and mechanical speed with MPPT and PITCH

Fig. 11 shows the simulation results for field-oriented control with a first order sliding mode regulator of the DFIG associated with a static converter integrated in a wind system when the reference steps of power were applied.

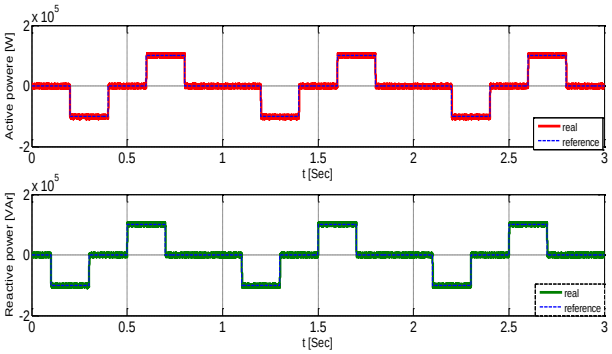

Figure 11. Active and reactive power

The wind generation system must extract the maximum wind power when the speed is lower than the nominal values [2]; this power corresponds to the active power generated by DFIG. The reactive power must be zero to ensure a unity power factor on the stator side. Fig.12 presents the estimated active power from the MPPT power (electromagnetic torque controlled by the MPPT algorithm and PITCH system) and reactive power.

We observe that the system extracts the nominal values of active power (1.5MW, maximum power can be generated by this system) regardless of the existing wind power. This power limitation is used to avoid a possible over-speed of the rotor and to protect the electrical system (the generator). When the wind speed decreases, the MPPT algorithm applies the maximized power extracted from the wind (1.5−2s).

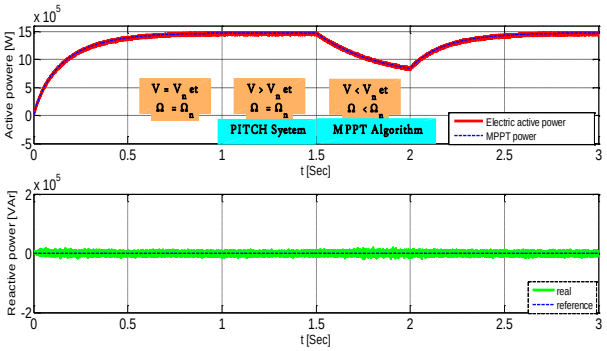

Figure 12. Power active estimated and reactive power zero

Fig. 13 presents the simulation results of MPPT and PITCH electromagnetic torque generated from the mechanical part as a reference (red), the electromagnetic torque developed by DFIG (blue), and the stator currents.

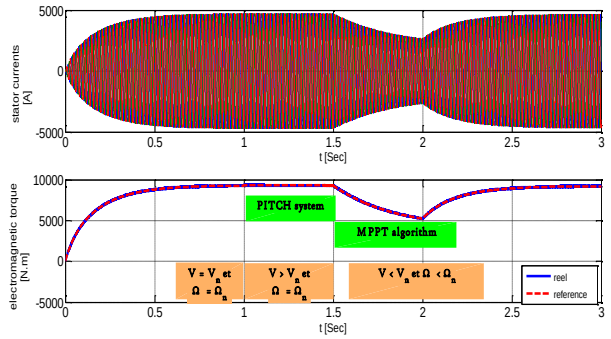

Figure 13. Electromagnetic torque and stator currents of the overall system

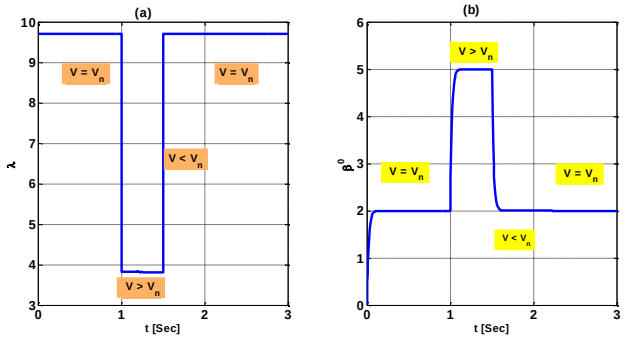

Figure 14. Variation of the relative speed and the angle

Fig. 14 presents the variation of the relative speed and the blade angle. Note that the wind speed is equal to the nominal value, the relative speed is equal to the optimum value $\boldsymbol{\lambda_{opt}}$, and $\boldsymbol{\beta}$ is equal to $\boldsymbol{\beta_{opt}}$. If the wind speed increases, the relative ration speed decreases and the angle timing increases (PITCH system). If the wind speed takes a value lower than the nominal value, then the relative velocity increases and returns to its optimal value.

6 Conclusions

Regulation by means of a first order sliding mode regulator shows a good performance even in the presence of changes in instructions. Decoupling ensures stability and convergence. In addition, this setting presents a very simple robust control algorithm.

The interest of the PITCH system in the protection of mechanical part and electric part (generator) is achieved when the rate of wind speed is exceeded.

The interest of the MPPT algorithm in the extraction of the maximum wind power is acquired when the speed of the wind is decreased such that a high power yield of the generation system is implied.

References:

[1] Belmokhtar K., Doumbia L. and Agbossou K. "*Modelling and control of a wind energy system down to supply power to the DFIM grid*" (French) , 4th International Conference on Electrical Engineering, CIGE'10. University of Bechar, Algeria. 03-04 November 2010.

[2] Beltran B. "*Contribution to the robust control of wind turbines based on DFIG: the classic sliding mode and higher order sliding mode*" (French). PhD thesis, University of Western Brittany, 2010.

[3] Bianchi FD., De Battista H. and Mantz RJ. "*Wind turbine control systems: principles, modelling and gain scheduling design*". Springer, London. 2007.

[4] Beltran B., Benbouzid MEH. and Ahmed-Ali T. "*High-order sliding mode control of a DFIG-based wind turbine for power maximization and grid fault tolerance*". In: Proceedings of IEEE IEMDC. Miami, USA. 2009.

[5] Bouhedda A. "*Contribution to the study of a wind turbine control systems*" (French). PhD thesis, University of Mouloud Mammeri. Tizi-Ouzou, Algeria, 2011.

[6] Poitiers F. "*Study and Control of asynchronous generators for the use in wind power*" (French). PhD thesis, Polytechnic School of Nantes, France, 2003.

[7] Cardenas R., Pena R., Alepuz S. and Asher G. "*Overview of control systems for the operation of DFIGs in wind energy aplications*". IEEE Trans Ind Electron, pp 2776-2798. 2013

[8] Itaso Martinez M., Susperregui A., Tapia G. and Camblong H. "*Sliding-Mode Control for a DFIG-based Wind Turbine under Unbalanced Voltage*". Preprints of the 18th IFAC Word Congress Milano (Italy). 2011.

[9] Hamdi N. "*Modeling and control of wind power generators*" (French). Magister thesis in Electrical Engineering, University of Mentouri, Algeria, 2008.

[10] Djeriri L. "*Vector control of a DFIM integrated in wind system*" (French). PhD thesis, University of Djilali Liabes of Sidi-Bel-Abbes, Algeria, 2008.

[11] Gaillard A. "*Wind turbine system based on a DFIM: Contribution to the study of the quality of electric power and continuity Service*" (French). PhD thesis, University of Henri Poincare Nancy I, France, 2010.

[12] Djilali L. "*FOC Comparative study of a wind power system a basis of DFIG with and without control of the mechanical part*" (French). 2nd International Conference on electronics, electrical and automatic. Oran, Algeria, 26-27 November 2013.

[13] Mejía D., Torres I., and Diaz J. *"MPPT control systems used in sunflower for maximum efficiency"*. Revista Colombiana de Tecnologías de Avanzada, pp. 118-123. ISSN: 1692-7257-Vol. 1.2016.

[14] Giménez M. *"Develop advance in new strategies for electric machine control base on DTC (Direct Torque Control)"*. Revista Colombiana de Tecnologías de Avanzada, pp. 27-36. ISSN: 1692-7257-Vol. 1.2007.
[15] Bachtarzi A. "*Control of variable structure systems Applications to a steam generator*" (French), PhD thesis, University of Constantine, Algeria. 2011.
[16] Beltran B., Benbouzid MEH. and Ahmed-Ali T. "*DFIG-based wind turbine robust control using high-order sliding modes and a high gain observer*". HAL archives-ouvertes. International Review on Modelling and Simulations, pp. 1148-1155. 2011.
[17] Bermeo W., Souza Jr A., Fernandes T., Honórico D., Nogueira L., and Barreto L. *"Sliding model control applied in current loop for a DSP-based position control applied to squirrel-cage induction motor"*. Revista Colombiana de Tecnologías de Avanzada, pp. 26-32. ISSN: 1692-7257-Vol. 1.2016.
[18] Utkin V., Guldner J. and Shi J. "*Sliding Mode Control in Electromechanical Systems*". Taylor&Francis, London, UK. 1999.
[19] Álvarez R., García M., and Torregoza A. *"Photovoltaic module-integrated converter (mic) based on semi-z-source inverters (szsi): a new sliding mode control scheme"*. Revista Colombiana de Tecnologías de Avanzada, pp. 61-66. ISSN: 1692-7257-Vol. 1.2014.